A feasibility trial of skin surface motion-gated stereotactic body radiotherapy for treatment of upper abdominal or lower thoracic targets using a novel O-ring gantry

Kendall Kiser [a,*], Joshua Schiff [a], Eric Laugeman [a], Taeho Kim [a], Olga Green [a,b], Casey Hatscher [a], Hyun Kim [a], Shahed Badiyan [a], Matthew Spraker [a,c], Pamela Samson [a], Clifford Robinson [a], Alex Price [a,d], Lauren Henke [a,d]

[a] Department of Radiation Oncology, Washington University in St. Louis School of Medicine, 660 S. Euclid Avenue, MSC 8224-35-LL, St. Louis, MO 63110, USA
[b] Varian Medical Systems, 3100 Hansen Way, Palo Alto, CA 94304, USA
[c] Centura Health, 2525 S Downing St., Denver, CO 80210, USA
[d] Department of Radiation Oncology, Case Western Reserve School of Medicine, 11100 Euclid Avenue, Cleveland, OH 44106, USA

ARTICLE INFO

ABSTRACT

Background and purpose: A novel O-ring gantry can deliver stereotactic body radiation therapy (SBRT) with artificial intelligence-facilitated, CT-guided online plan adaptation. It gates mobile targets by optically monitoring skin surface motion. However, this gating solution has not been clinically validated. We conducted a trial to evaluate the feasibility of optical skin surface-guided gating for patients with mobile upper abdominal or lower thoracic malignancies treated with SBRT on this platform (NCT05030454).
Materials and methods: Ten patients who were prescribed SBRT to a thoracic or abdominal target and were capable of breath-hold for at least 17 s enrolled. They received SBRT in five fractions with breath-hold technique and optical skin surface motion monitored-gating with a $\pm$ 2 mm tolerance. Online plan adaptation was left to the discretion of the daily treating physician. The primary endpoint was defined as successful completion of > 75 % of attempted fractions. Exploratory endpoints included local control and acute grade $\geq$ 3 toxicity rates after three months. For adapted fractions the contouring, planning, quality assurance, and treatment delivery times were recorded.
Results: Forty-seven of 51 SBRT fractions (92 %) were successfully gated at breath-hold by optical skin surface motion monitoring. The tumor centroid position during breath-hold varied by a mean of approximately 2 mm. Sixty-three percent of fractions were adapted online with a median total treatment time of 78.5 min. After three months no local recurrences or acute grade $\geq$ 3 toxicities were observed.
Conclusions: SBRT treatment to mobile targets with surface-monitored gating on a novel O-ring gantry was prospectively validated.

Introduction

Stereotactic body radiation therapy (SBRT) involves the delivery of high doses of radiation per fraction using advanced tumor localization techniques. Ablative doses achieved by SBRT increase the probability of local tumor control in numerous cancer types [1–8]. For example, SBRT has demonstrated favorable local control in early stage non-small cell lung cancer (NSCLC) and is now a standard of care form of radiotherapy delivery for inoperable early stage lung cancer patients [9,10].

However, SBRT demands the utmost precision and accuracy to protect organs-at-risk (OARs) since acute and late toxicities can annul the benefit of the treatment [11–13]. In the lower thorax and upper abdomen, respiratory, digestive, and cardiovascular motion introduce particular OAR positional uncertainty, yet certain malignancies that arise in these anatomic regions – such as non-small cell lung cancer [14,15] and pancreatic adenocarcinoma [2,16,17] – may have improved control with SBRT compared to conventionally fractionated radiotherapy. Hence accurate intra-fraction motion management is necessary

for safe and efficacious ablative radiotherapy in these disease sites.

A novel O-ring gantry capable of delivering SBRT to lower thoracic and upper abdominal malignancies with artificial intelligence-facilitated online plan adaptation was recently commercialized (Ethos; Varian Medical Systems, Palo Alto, CA). To manage intra-fraction motion, Ethos relies on IDENTIFY (Varian Medical Systems, Palo Alto, CA), which is an optical skin surface monitoring system equipped with multiple stereo-vision cameras to facilitate surface-guided radiotherapy (SGRT) [18]. However, an SGRT workflow for SBRT gating with Ethos has not yet been clinically demonstrated [19]. Therefore, we conducted a phase I clinical trial designed to evaluate the feasibility and safety of SGRT to lower thoracic and upper abdominal malignancies on the Ethos platform.

Methods and materials

Patient population

Between October 2021 and March 2022, ten patients with a biopsy-proven or radiographically diagnosed primary or metastatic cancer in the abdomen or lower thorax were enrolled on this prospective clinical trial (NCT05030454). This trial was approved by the Human Research Protection Office of the Washington University in St. Louis School of Medicine (IRB #202107198).

Eligible patients were at least 18 years of age, had a Karnofsky Performance Status of greater than 60, and had at least one site of disease suitable for SBRT in the lower thorax or upper abdomen per the treating radiation oncologist. Because patients were treated using deep end-inspiratory or end-expiratory breath-hold technique, eligible patients were also required to be able to hold their breath for 17 s. Patients were required to have completed systemic therapy at least one week prior to radiation and to refrain from treatment with systemic therapy for at least one week following completion of radiation. Patients were not eligible if they had prior radiotherapy in the projected treatment field, were undergoing treatment with an investigational agent, had an uncontrolled concurrent illness, or were pregnant.

Prescription

Trial protocol required SBRT delivery in five fractions of no less than 7 Gy per fraction. A gross tumor volume (GTV) or clinical target volume (CTV) delimited by the treating physician was symmetrically expanded 5 mm to make a planning target volume (PTV). No internal target volume (ITV) expansion was utilized because all treatments were planned at inhale or exhale breath-hold position. For patients undergoing non-adaptive SBRT, the prescription was delivered to the PTV. For patients undergoing CT-guided stereotactic adaptive radiotherapy (CT-STAR) per the treating physician's discretion, the prescription was delivered to the optimized planning target volume (PTVopt) to maximize target coverage within inviolable OAR constraints. The PTVopt was defined by trimming any PTV within 5 mm of critical OARs, as has been previously described [20].

Initial planning

Each patient underwent an initial simulation with a free-breathing 4D-CT and either an end-inspiratory or end-expiratory breath-hold CT. Intravenous and oral contrast agents were used to identify normal vascular and luminal structures, per physician discretion. Patients prescribed CT-STAR also underwent an Ethos kilovoltage (kV) cone beam CT (CBCT) to confirm the kV CBCT's suitability for daily adaptation. Patients with abdominal disease were positioned with one arm up and the other down in custom immobilization devices, while those with lower thoracic disease were positioned with both arms up, per our institutional SBRT practice.

Adaptive planning

For patients receiving CT-STAR, the Ethos adaptive workflow has previously been described [21]. Briefly, the initial plan (P_I) dose distribution was superimposed on the patient's kV CBCT anatomy-of-the-day. If the P_I delivered excessive dose to OARs or insufficient dose to the target, then the platform's artificial intelligence-driven treatment planning system (TPS) facilitated online creation of an adapted plan (P_A). Our institutional practice is to treat with P_A if P_A resolves an OAR constraint violation or safely improves target coverage by five percent or more. Re-optimization of dose deposition prioritized OAR hard constraints above target coverage. OAR constraints are described in Table 1.

Set-up and motion management

The IDENTIFY system is auxiliary to the Ethos treatment delivery system and does not have a stereotactic room reference. To correlate skin and internal anatomic positions, IDENTIFY must acquire a skin surface reference region-of-interest (ROI) in the treatment (breath-hold) position while a kV CBCT is simultaneously acquired. Patients were set up to skin marks using an in-bore laser system and then shifted to treatment isocenter. At isocenter patients were coached into a breath-hold and IDENTIFY acquired a reference ROI. Specifically, the ROI was selected by tracing a triangular pattern along the patient's rib cage beginning at the xiphoid process. IDENTIFY outputted the best signal when the skin topographic gradient comprised prominent three-dimensional features. IDENTIFY informed the therapy team when enough features were present to establish a reference ROI. A ± 2 mm gating boundary was then generated about the reference ROI and several repeat breath-holds were performed to determine if the position was reproducible. If so, the patient was coached once again into breath-hold position, a kV CBCT was acquired (Fig. 1A), and an updated reference surface was simultaneously captured (Fig. 1B) to link the surface and internal anatomic positions.

In fractions considered for adaptation, the steps of contouring, optimization, and QA were performed (Fig. 1C-E), and thereafter a verification CBCT was acquired to ensure the patient's anatomy had not substantially shifted during re-planning. During treatment delivery, IDENTIFY's tracing was monitored by the treatment team for manual gating. Further CBCTs were acquired after each arc in volumetric modulated arc therapy (VMAT) plans and at the completion of each fraction to verify patient positioning during and after treatment (Fig. 1F).

As described in full detail in a separate physics manuscript under review [22] we also sought to evaluate tumor residual motion during breath-hold and correlate this with skin surface residual motion. Here, we report key clinical evaluations. To determine tumor residual motion, 120 intra-fractional CBCTs acquired during SGRT breath-hold were manually aligned with positional reference breath-hold CBCTs acquired at the beginning of each fraction. Tumor residual motion was then

Table 1
Planning constraints.

Organ-at-Risk	Constraint
Stomach	V 3300 cGy $\leq$ 0.5 cc
Duodenum	V 3300 cGy $\leq$ 0.5 cc
Large intestine	V 3300 cGy $\leq$ 0.5 cc
Small Bowel	V 3300 cGy $\leq$ 0.5 cc
Kidneys	Mean $\leq$ 1500 cGy
Spinal Cord	D 0.5 cc $\leq$ 2500 cGy
Esophagus	D 0.03 cc < 3500 cGy
Esophagus	D 5 cc < 1950 cGy
Lungs	V 1350 cGy < 37 %
Trachea/Bronchus	D 0.03 cc < 4000 cGy
Trachea/Bronchus	D 5 cc < 3200 cGy
Heart	D 0.03 cc < 3800 cGy
Heart	D 15 cc < 3200 cGy
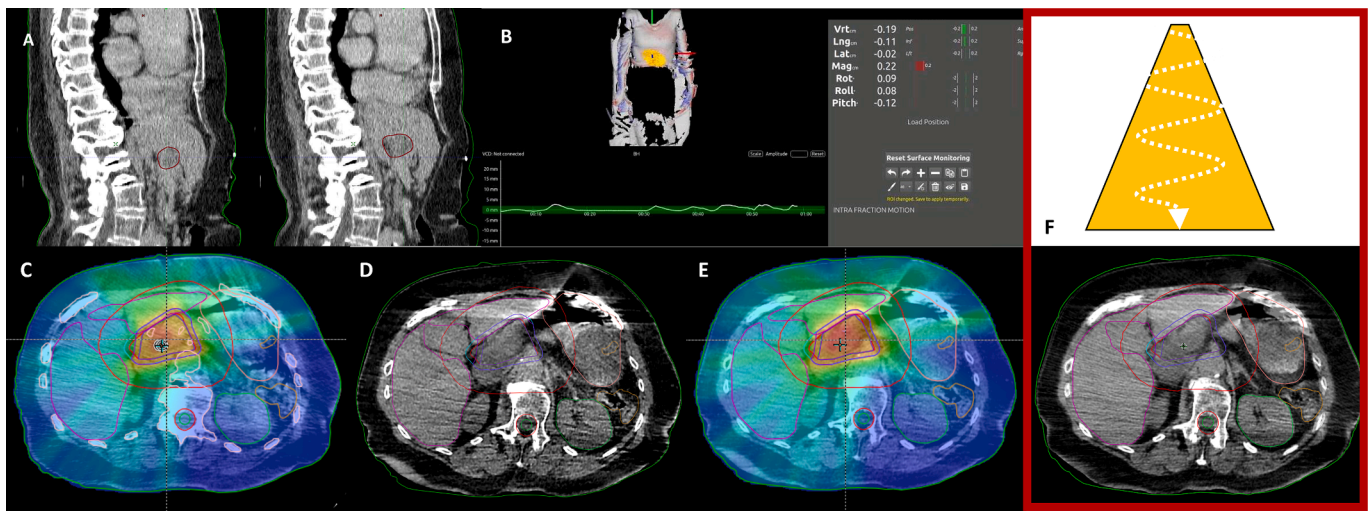
Fig. 1. A) End-inhale (left) and end-exhale (right) sagittal kV CBCT slices exemplify target motion in the superior/inferior dimension in one patient with pancreatic adenocarcinoma. B) A stereotactic map of the abdomen and chest surface of the patient from Fig. 1A. A skin ROI was selected (in yellow) and a respiratory trace monitoring the ROI was acquired. Beam delivery to the pancreatic target was manually halted if the ROI deviated outside a $\pm$ 2 mm gating boundary. C-E) In patients who underwent online adaptation, the original radiation plan was projected on a CBCT of the patient's anatomy-of-the-day (C), the patient's anatomic structures were re-contoured (D), and re-optimization and quality assurance were performed (E). F) Regardless of whether the patient was treated with or without online adaptation, the patient's position during SBRT beam-on was monitored by SGRT and confirmed by verification CBCTs acquired at regular intervals (including after each VMAT arc).

calculated as the difference in GTV centroid coordinate positions between intra-fractional CBCTs and their respective reference CBCTs. CTV centroids were substituted in patients without grossly identifiable tumor volumes. We also calculated dosimetric changes due to tumor residual motion by registering pre-arc CBCTs to their respective reference CBCTs and radiation plan.

Endpoints

This trial's primary endpoint was feasibility, which was defined as successful delivery of SBRT to abdominal or lower thoracic targets using IDENTIFY SGRT in greater than 75 % of scheduled fractions. Six exploratory endpoints were defined a priori: 1) calculation of geometric agreement between patient skin and tumor positions in surface-monitored, intra-fractional breath-hold CBCT image sets, 2) determination of minimal PTV margins to be used with SGRT, 3) comparison of the SGRT system with a standard-of-care respiratory gating system, 4) local control rates at three months using Response Evaluation Criteria in Solid Tumours (RECIST) version 1.1, 5) acute (within 90 days) grade $\geq$ 3 toxicity rates using Common Terminology Criteria for Adverse Events version 5.0 (CTCAE v 5.0), and 6) qualitative description of patient factors that might interfere with surface imaging tracking, such as patient surface topography or skin tone.

Data collection and statistics

Clinical data were recorded prospectively at the time of each patient consultation, and toxicities were collected during radiation and three months post-SBRT. Local control rates were assessed at three months post-SBRT. Dosimetric data were likewise recorded prospectively during each treatment fraction. For fractions that underwent online adaptation, logistical re-planning data were recorded.

Results

Clinical characteristics of the ten treated patients are summarized in Table 2. The median patient age was 72, all had Eastern Cooperative Oncology Group (ECOG) performance statuses $\leq$ 1, and most were female (70 %). Patient races were Caucasian (80 %), Asian (10 %), and

Table 2

Patient characteristics. Qualitative data are counts. Quantitative data are means with ranges in parentheses.

Age	70.1 years (40–86)	
Gender	Male	3
	Female	7
ECOG score	0	5
	1	5
Site	Pancreas	6
	Retroperitoneum	1
	Lung	1
	Liver	1
	Bile duct	1
Stage	I	2
	II	1
	III	1
	IV	5
	Indeterminate	1
Tumor volume	37.9 cm^3 (2.3–68.3)	
Body mass index	29.8 kg/m^2 (21.96–40.24)	
Race	White	8
	Asian	1
	Black	1
Abdominal hair	None	7
	Present	3
Comorbidities at risk of complicating treatment	Arthritis or positional pain	3
	Chronic obstructive pulmonary disorder	2
	Heart failure	3
	Arrhythmias	5
	Frontotemporal dementia	1
Respiratory treatment phase	End-inhale	3
	End-exhale	7
4D simulation CT superior/inferior motion	1.26 cm (0.6–2.6)	

Black (10 %). Patient cancer histologies were pancreatic adenocarcinoma (50 %), non-small cell lung cancer, colon adenocarcinoma (10 %), liposarcoma (10 %), and cholangiocarcinoma (10 %). Half of patients had stage IV disease. In 80 % of patients the SBRT target was the primary lesion; the remaining targets were comprised of metastatic lesions in the liver (10 %) or pancreas (10 %). All but two patients had at least one

medical comorbidity with potential to impede the feasibility of SGRT, including respiratory and cardiovascular comorbidities that could impair breath-hold (60 %), musculoskeletal, autoimmune, or neurogenic back or abdominal positional pain (30 %), and frontotemporal dementia (10 %). Forty percent of patients had an implanted pacemaker or cardioverter defibrillator, none of which were proximal to the lower thorax or upper abdominal SBRT sites. The median patient BMI was 29.8 kg/m^2. Thirty percent of patients had chest and/or abdominal hair. One patient's chest had numerous seborrheic keratoses, and another patient had bilateral breast reconstructions.

The number of fractions successfully delivered with SGRT was 47 of 51 fractions (92 %). The total number of fractions was 51 rather than 50 because one patient tolerated only partial delivery of his first fraction due to positional pain. However, the undelivered dose was successfully delivered in a sixth/completion fraction. In three fractions there was an IDENTIFY SGRT software outage, twice midway through a fraction and once prior to a fraction initiation. In these instances each fraction was still successfully delivered using a backup respiratory motion management system [23]. Each software outage was resolved before the subsequent fraction and there were no treatment delays. The median total fraction time was 78.5 min for all fractions (IQR 63–95 min), 91.5 min for adapted fractions (IQR 79–103 min), and 51.5 min for non-adapted fractions (IQR 45–64 min).

All patients except one were treated to a nominal dose of 50 Gy in 5 fractions to the PTVopt. The exception was treated to a nominal dose of 55 Gy in 5 fractions. At three months no patient had been lost to follow-up, and the local control rate for all targets was 100 %. Fifty percent of patients had distant disease progression, including in the liver (40 %) and in the adrenal and peritoneum (10 %). The treatment-related CTCAE grade $\geq$ 3 toxicity rate was 0 %.

Residual tumor motion during breath hold was 1.8 ± 1.8 mm (mean ± standard deviation) in the superior/inferior dimension, 2.0 ± 2.2 mm in the medial/lateral dimension, and 2.0 ± 1.8 mm in the anterior/posterior dimension (Fig. 2). This was not significantly different between patients treated at end-exhale or end-inhale. Skin surface residual motion was 2.3 ± 2.1 mm in the superior/inferior dimension, 2.5 ± 2.0 mm in the medial/lateral dimension, and 2.0 ± 2.3 mm in the anterior/posterior dimension. The most extreme residual motion deviations were 14 mm and 12 mm in the medial/lateral dimension, and both were observed in the same fraction. Tumor residual motion changed the percentage of GTV (or CTV in cases where a CTV was used) covered by prescription dose by a mean of −2.8 % ± 4.4 %.

Sixty-three percent (32/51) of fractions were adapted. The median times to re-contour and re-plan (including quality assurance checks)

Table 3
Online adaptation times. Data are median times with interquartile ranges in parentheses.

Adaptation time	Re-contour	16 min (10–20.5)
	Re-plan	11 min (9.5–13.5)
	Delivery	28 min (22–34.5)
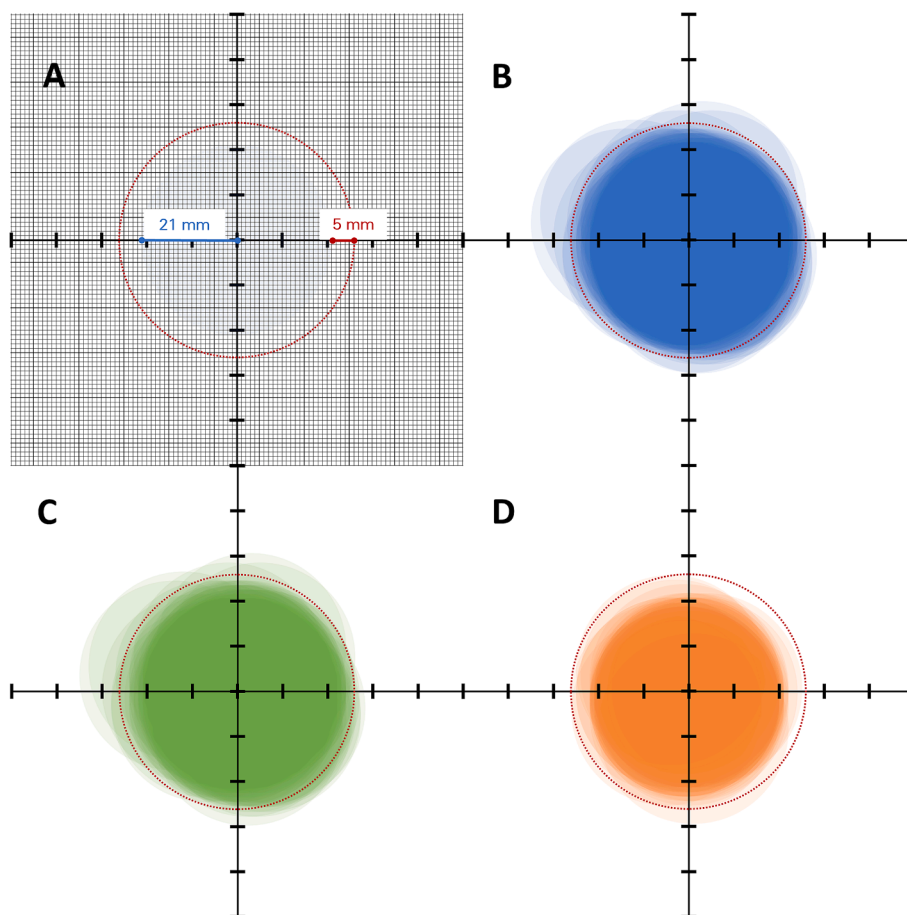
Fig. 2. A) Transparent circles visualize tumor residual motion in the medial/lateral (x) and anterior/posterior (y) axes in 120 intra-fractional CBCTs acquired during skin surface optically monitored breath-hold. Each circle has a radius of 21 mm, the radius of a sphere that is volumetrically equivalent to the mean gross tumor volume observed in this study. The axes' origin represents the tumor centroid coordinate position in reference CBCTs acquired at the beginning of each fraction. The dotted red circle frames the tumor with a 5 mm PTV margin. B) Tumor positions in all end-exhale and end-inhale CBCTs. C) Tumor positions in end-exhale CBCTs only (n = 87 CBCTs from seven patients). D) Tumor positions in end-inhale CBCTs only (n = 33 CBCTs from three patients).

were 16 and 11 min, respectively, and the median delivery time (including verification CBCTs between arcs) was 28 min (Table 3). Among twenty-eight adapted fractions with available data, 54 % both resolved an OAR constraint violation and improved PTVopt coverage, 39 % resolved OAR constraint violations alone, and 7 % improved PTVopt coverage alone. In adapted fractions the OARs most likely to need adaptation were the stomach (71 %), small bowel (57 %), duodenum (43 %), and large bowel (39 %).

When indicated and performed, adaptation decreased the median V33Gy to stomach by 3.0 cc, to small bowel by 1.1 cc, to large bowel by 0.4 cc, and to duodenum by 0.2 cc (Fig. 3A). Although the spinal cord and kidney dose constraints were never violated, adaptation minimally decreased the median dose to 0.5 cc of the spinal cord by 33 cGy and minimally increased the median mean kidney dose by 9 cGy. Adaptation increased the median dose to 95 % of the PTVopt volume by 3.72 Gy (from 47.3 Gy (94.6 % of prescription dose) to 51.0 Gy (102.1 % of prescription dose)) and the median percentage of the PTVopt volume that received 95 % of the prescription dose by 4.3 % (from 94.9 % to 99.2 %) (Fig. 3B).

Discussion

Recent best-practice guidelines from the American Association of Physicists in Medicine (AAPM) [24] and the European Society of Therapeutic Radiology and Oncology (ESTRO) [19] highlight the need to clinically validate the use of SGRT in emerging clinical use cases. In keeping with this recommendation, the phase I trial results presented here support the feasibility of IDENTIFY SGRT for SBRT treatment to upper abdominal and lower thoracic malignancies using a novel O-ring linear accelerator. All but four planned SBRT fractions were delivered with SGRT guidance, which met our pre-specified feasibility threshold of treatment delivery in 75 % of fractions. At a follow-up interval of three months, no patient had suffered disease progression at the irradiated site or a treatment-related grade ≥ 3 toxicity.

As a secondary endpoint we explored what magnitude of skin surface and tumor residual motion may be expected during breath-hold. In a separate, forthcoming manuscript [22] we found that tumor residual motion and skin surface residual motion were small and of similar magnitudes, averaging approximately 2 mm. Dosimetric deviations due to tumor residual motion were small. This encourages us that a 5 mm PTV expansion reasonably accounted for tumor residual motion in our cohort. Despite this, the most extreme residual motion deviations in our study were 14 mm and 12 mm and were both observed in the same fraction, highlighting the possibility of unacceptably high deviations given patient anatomy-of-the-day or compliance with treatment protocol on a given day.

The magnitude of tumor residual motion we observed was comparable to that reported by Dawson et al. [25] in each dimension: 1.8 mm vs. 2.2 mm superior/inferior, 2.0 mm vs. 2.0 mm medial/lateral, and 2.0 vs. 2.0 mm anterior/posterior. Dawson et al. delivered SBRT to liver targets with exhale breath-hold technique, but patient breathing cycles were externally controlled by an active breathing control device rather than monitored by SGRT, and daily image guidance consisted of megavoltage anterior/posterior and lateral portal images rather than CBCTs. In contrast to our results, Zeng et al. [26] reported larger magnitudes of tumor residual motion in the superior/inferior dimension, with per patient averages of 3–21 mm. Zeng et al. delivered hypo- and conventionally fractionated radiation with TrueBeam linacs (Varian Medical Systems, Palo Alto, CA) to 13 pancreatic targets and 1 liver target with inspiratory breath-hold gated by AlignRT optical skin surface guidance (Vision RT, London, UK). The differences between the results reported by this study and ours may be contributed to by differences in skin surface motion gating tolerance (± 3 mm vs. ± 2 mm), the selection of ROI (an abdominal ROI at least 20 cm $\times$ 15 cm vs. a sub-xiphoid ROI optimized for prominent three-dimensional features), the treatment breath-hold phase (exclusively inspiration vs. exclusively expiration for
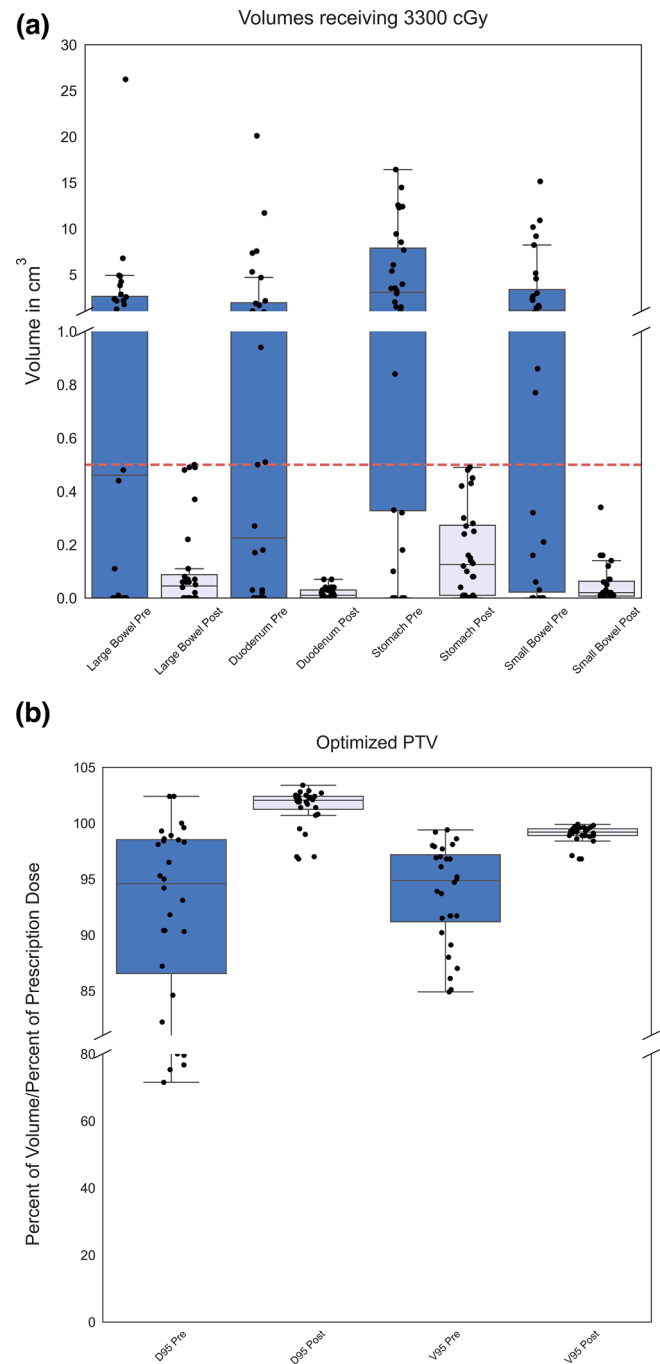
Fig. 3. A) Volumes of luminal organs-at-risk that would receive 3300 cGy preadaptation (blue) and post-adaptation (lavender). The red line demarcates the dose constraint for all luminal organs at risk: V3300 cGy ≤ 0.5 cc. B) Percentage of prescription dose to 95 % of the PTVopt volumes (D95) or percentages of the PTVopt receiving 95 % of the prescription dose (V95) pre-adaptation (blue) and post-adaptation (lavender). Box lines represent lower quartile, median, and upper quartile values, while whiskers represent minimum and maximum values. Points beyond the upper or lower whisker are greater than 1.5 times the interquartile range from the upper or lower quartile.

pancreatic targets), the methodology for assessing tumor position (*peri*-tumoral fiducial marker position in 2D kV images acquired during real-time beam delivery every $20° − 40°$ of gantry rotation vs. tumor centroid position in pre-beam-on verification CBCTs), or the frequency of assessment (typically 27 images per fraction vs. typically 2–3 CBCTs per fraction).

An advantage of the Ethos platform is its capability to produce SBRT

plans adapted to a patient's anatomy-of-the-day. Online adaptation was not required by the trial protocol, but over half of the fractions delivered underwent adaptation, and nearly all adaptations were motivated by OAR constraint violations. The frequency of OAR violations was comparable to that reported in prior experiences with online adaptive RT [20,27]. While this sample size is small, the absence of acute grade ≥ 3 toxicity demonstrated in this study provides encouraging early safety data for the delivery of CT-STAR to the thorax and abdomen. Further clinical trials designed to establish the clinical significance of the incremental dosimetric improvements made possible by modern online adaptation technologies are needed.

This prospective clinical trial has limitations. We developed a backup breath-hold visualization system in-house in case SGRT system malfunctioned, and it was needed to successfully deliver treatment in three fractions. Twice (in the same patient) SGRT malfunctioned midway through a fraction. In a third instance (with a separate patient) the SGRT system did not function at any point during the fraction. This illustrates the utility of a contingency system to avoid unplanned treatment delays or cancellations. Second, our sample size was small and follow-up was short. This was appropriate for our primary feasibility endpoint, but limits conclusions with respect to toxicity and efficacy. Notwithstanding the small sample size, variations in skin tone, hair, body mass, and female breast shape did not appear to impede SGRT.

Conclusions

IDENTIFY SGRT to facilitate Ethos SBRT to abdominal and lower thoracic targets was successfully delivered in 92 % of fractions, which met this trial's primary feasibility endpoint and remained feasible even when online adaptation was employed. At three months, no patient had progressed locally at the treated disease site or suffered a treatment-related grade 3 toxicity. To our knowledge, this is the first clinical validation of SGRT for Ethos SBRT treatment of lower thoracic or upper abdominal malignancies.

Conflicts of interest

JS has received grant support from Varian Medical Systems. **OG** has received speaker fees from ViewRay. **HK** has received grant support from ViewRay and Varian Medical Systems and speaker fees from Varian Medical Systems. **SB** has received honoraria from Mevion. **MS** has received grant support from Varian Medical Systems and the Emerson Foundation and honoraria from Varian Medical Systems. **PS** has received honoraria from Varian Medical Systems and Astra Zeneca. **CR** has received grant support from Varian Medical Systems and Merck, royalties from Varian Medical Systems, consulting fees from Varian Medical Systems, Astra Zeneca, EMD Serono, Radialogica, and Quataras and has stock in Radialogica and Quantaras. **AP** has received grant support from Varian Medical Systems and travel support from ViewRay and Sun Nuclear Corporation. **LH** has received grant support from Varian Medical Systems, consulting fees from Varian Medical Systems, honoraria from Varian Medical Systems and ViewRay, and travel support from LusoPalex.

Funding statement

Author contributions

LH, EL, TK, PS, CR, and AP conceived the trial and wrote its protocol. LH, HK, SB, MS, PS, CR, KK, JS, and CH accrued patients to the trial. EL, TK, OG, and AP oversaw the physics. CH coordinated patient follow-up. KK, EL, TK, AP, and LH analyzed and collected the data. KK wrote the manuscript, which all authors reviewed and approved.

Declaration of Competing Interest

The authors declare that they have no known competing financial interests or personal relationships that could have appeared to influence the work reported in this paper.

Acknowledgements

References

[1] Ball D, Mai GT, Vinod S, et al. Stereotactic ablative radiotherapy versus standard radiotherapy in stage 1 non-small-cell lung cancer (TROG 09.02 CHISEL): a phase 3, open-label, randomised controlled trial. Lancet Oncol 2019;20(4):494–503. https://doi.org/10.1016/s1470-2045(18)30896-9.

[2] Hassanzadeh C, Rudra S, Bommireddy A, et al. Ablative Five-Fraction Stereotactic Body Radiation Therapy for Inoperable Pancreatic Cancer Using Online MR-Guided Adaptation. Adv Radiat Oncol 2021;6(1):100506. https://doi.org/10.1016/j.adro.2020.06.010.

[3] Henke LE, Stanley JA, Robinson C, et al. Phase I Trial of Stereotactic MRI-Guided Online Adaptive Radiation Therapy (SMART) for the Treatment of Oligometastatic Ovarian Cancer. Int J Radiat Oncol Biol Phys 2022;112(2):379–89. https://doi.org/10.1016/j.ijrobp.2021.08.033.

[4] Kalbasi A, Kamrava M, Chu FI, et al. A Phase II Trial of 5-Day Neoadjuvant Radiotherapy for Patients with High-Risk Primary Soft Tissue Sarcoma. Clin Cancer Res 2020;26(8):1829–36. https://doi.org/10.1158/1078-0432.CCR-19-3524.

[5] Palma DA, Olson R, Harrow S, et al. Stereotactic Ablative Radiotherapy for the Comprehensive Treatment of Oligometastatic Cancers: Long-Term Results of the SABR-COMET Phase II Randomized Trial. J Clin Oncol 2020;38(25):2830–8. https://doi.org/10.1200/JCO.20.00818.

[6] Vicini FA, Cecchini RS, White JR, et al. Long-term primary results of accelerated partial breast irradiation after breast-conserving surgery for early-stage breast cancer: a randomised, phase 3, equivalence trial. Lancet 2019;394(10215):2155–64. https://doi.org/10.1016/s0140-6736(19)32514-0.

[7] Chin RI, Roy A, Pedersen KS, et al. Clinical Complete Response in Patients With Rectal Adenocarcinoma Treated With Short-Course Radiation Therapy and Nonoperative Management. Int J Radiat Oncol Biol Phys. Oct 12 2021;doi:10.1016/j.ijrobp.2021.10.004.

[8] Jang WI, Bae SH, Kim MS, et al. A phase 2 multicenter study of stereotactic body radiotherapy for hepatocellular carcinoma: Safety and efficacy. Cancer 2020;126(2):363–72. https://doi.org/10.1002/cncr.32502.

[9] Timmerman R, Paulus R, Galvin J, et al. Stereotactic body radiation therapy for inoperable early stage lung cancer. J Am Med Assoc 2010;303(11):1070–6. https://doi.org/10.1001/jama.2010.261.

[10] National Comprehensive Cancer Network. Non-Small Cell Lung Cancer (Version 5.2022). Accessed 11/7/2022, https://www.nccn.org/professionals/physician_gls/pdf/nscl.pdf.

[11] Koong AC, Christofferson E, Le QT, et al. Phase II study to assess the efficacy of conventionally fractionated radiotherapy followed by a stereotactic radiosurgery boost in patients with locally advanced pancreatic cancer. Int J Radiat Oncol Biol Phys 2005;63(2):320–3. https://doi.org/10.1016/j.ijrobp.2005.07.002.

[12] Timmerman R, McGarry R, Yiannoutsos C, et al. Excessive toxicity when treating central tumors in a phase II study of stereotactic body radiation therapy for medically inoperable early-stage lung cancer. J Clin Oncol 2006;24(30):4833–9. https://doi.org/10.1200/JCO.2006.07.5937.

[13] Haseltine JM, Rimner A, Gelblum DY, et al. Fatal complications after stereotactic body radiation therapy for central lung tumors abutting the proximal bronchial tree. Pract Radiat Oncol 2016;6(2):e27–33. https://doi.org/10.1016/j.prro.2015.09.012.

[14] Onishi H, Araki T, Shirato H, et al. Stereotactic hypofractionated high-dose irradiation for stage I nonsmall cell lung carcinoma: clinical outcomes in 245 subjects in a Japanese multiinstitutional study. Cancer 2004;101(7):1623–31. https://doi.org/10.1002/cncr.20539.

[15] Nyman J, Hallqvist A, Lund JA, et al. SPACE - A randomized study of SBRT vs conventional fractionated radiotherapy in medically inoperable stage I NSCLC. Radiother Oncol Oct 2016;121(1):1–8. https://doi.org/10.1016/j.radonc.2016.08.015.

[16] Chuong MD, Bryant J, Mittauer KE, et al. Ablative 5-Fraction Stereotactic Magnetic Resonance-Guided Radiation Therapy With On-Table Adaptive Replanning and Elective Nodal Irradiation for Inoperable Pancreas Cancer. Pract Radiat Oncol 2021;11(2):134–47. https://doi.org/10.1016/j.prro.2020.09.005.

[17] Krishnan S, Chadha AS, Suh Y, et al. Focal Radiation Therapy Dose Escalation Improves Overall Survival in Locally Advanced Pancreatic Cancer Patients Receiving Induction Chemotherapy and Consolidative Chemoradiation. Int J Radiat Oncol Biol Phys 2016;94(4):755–65. https://doi.org/10.1016/j.ijrobp.2015.12.003.

[18] Nguyen D, Farah J, Barbet N, Khodri M. Commissioning and performance testing of the first prototype of AlignRT InBore a Halcyon and Ethos-dedicated surface guided radiation therapy platform. Phys Med Dec 2020;80:159–66. https://doi.org/10.1016/j.ejmp.2020.10.024.

[19] Freislederer P, Batista V, Ollers M, et al. ESTRO-ACROP guideline on surface guided radiation therapy. *Radiother Oncol*. May 31 2022;doi:10.1016/j. radonc.2022.05.026.

[20] Schiff JP, Price AT, Stowe HB, et al. Simulated computed tomography-guided stereotactic adaptive radiotherapy (CT-STAR) for the treatment of locally advanced pancreatic cancer. Radiother Oncol Oct 2022;175:144–51. https://doi.org/ 10.1016/j.radonc.2022.08.026.

[21] Schiff JP, Stowe HB, Price A, et al. In Silico Trial of Computed Tomography-Guided Stereotactic Adaptive Radiation Therapy (CT-STAR) for the Treatment of Abdominal Oligometastases. *Int J Radiat Oncol Biol Phys*. Jun 26 2022;doi:10.1016/ j.ijrobp.2022.06.078.

[22] Kim T, Laugeman E, Kiser KJ, et al. Surface imaging for Cone Beam Computed Tomography-guided StereoTactic Adaptive/Body Radiotherapy: intra-fractional breath-hold motion management. Med Phys (in Submission) 2023.

[23] Kim T, Ji Z, Lewis B, et al. Visually guided respiratory motion management for Ethos adaptive radiotherapy. J Appl Clin Med Phys Jan 2022;23(1):e13441.

[24] Al-Hallaq HA, Cervino L, Gutierrez AN, et al. AAPM task group report 302: Surface-guided radiotherapy. Med Phys Apr 2022;49(4):e82–112. https://doi.org/ 10.1002/mp.15532.

[25] Dawson LA, Eccles C, Bissonnette JP, Brock KK. Accuracy of daily image guidance for hypofractionated liver radiotherapy with active breathing control. Int J Radiat Oncol Biol Phys 2005;62(4):1247–52. https://doi.org/10.1016/j. ijrobp.2005.03.072.

[26] Zeng C, Lu W, Reyngold M, et al. Intrafractional accuracy and efficiency of a surface imaging system for deep inspiration breath hold during ablative gastrointestinal cancer treatment. J Appl Clin Med Phys Nov 2022;23(11):e13740.

[27] Henke L, Kashani R, Robinson C, et al. Phase I trial of stereotactic MR-guided online adaptive radiation therapy (SMART) for the treatment of oligometastatic or unresectable primary malignancies of the abdomen. Radiother Oncol Mar 2018; 126(3):519–26. https://doi.org/10.1016/j.radonc.2017.11.032.